# Hydrogen Generation from Methanol Oxidation on Supported Cu and Pt Catalysts

*Yu-Chuan Lin[a], Keith L. Hohn[a, *], Susan M. Stagg-Williams [b]*

[a] Department of Chemical Engineering, Kansas State University,
   105 Durland Hall, Manhattan, KS 66502-5102, USA
[b] Chemical and Petroleum Engineering Department, University of Kansas,
   4132 Learned Hall, Lawrence, KS 66045-7609, USA

---

[*] Corresponding author's Tel.: +1-785-532-4315; Fax: +1-785-532-7372; E-mail: hohn@cheme.ksu.edu

## 1. Introduction

Methanol is a chemical of vital importance as a building block of various compounds and materials, such as acetic acid, methyl formate or N-N dimethyl formamide. Lately, it has also been viewed as a source of hydrogen-rich liquid carrier, which can be oxidized to form hydrogen via catalytic partial oxidation (CPO). This not only overcomes the difficulty of the storage/refueling of hydrogen, but also provides a convenient way for on-board hydrogen generation on the fuel cell powered automobiles.

Hydrogen generation from CPO of alcohols have been studied on various types of catalysts, among them, the most encountered are supported copper, palladium and platinum catalysts. Copper containing catalysts [1-4] give similar results as supported palladium catalysts [5-8] for CPO of methanol. Both of them produce primarily $H_2$ and $CO_2$, but also deactivate over time. Recently, CPO of methanol and ethanol have been studied on platinum catalysts [9-14]. Platinum catalysts have the advantage of being stable, unlike copper and palladium-containing catalysts, but produce much more CO, which is a disadvantage since CO is toxic, and known to be the poison of the proton exchange membrane (PEM) fuel cell anode.

The mechanism of methanol partial oxidation over copper and platinum is not well understood. Multiple reactions may play a role in a catalytic partial oxidation reactor, including catalytic partial oxidation (CPO), methanol decomposition (MD), methanol steam reforming (MSR), and the water-gas shift (WGS). An understanding of which reaction pathways are important is critical for designing better catalysts in methanol CPO processors. In this work, the mechanism of methanol CPO was studied over copper and platinum catalysts with the objectives of determining which reaction pathways are important and why copper and platinum give much different product distributions.

## 2. Experimental

2.1 Catalyst preparation

The catalyst comprising 40wt% of Cu supported on ZnO was prepared via the co-precipitation method [15,16]. This weight percent of Cu has been reported to have the highest activity among other compositions [1,17]. The synthesis procedure was as follows: aqueous solutions of two nitrate salts were prepared, one by dissolving 8.4 g of $Cu(NO_3)_2$ into 300 mL of deionized water and the other by dissolving 13 g of $Zn(NO_3)_2$ into the same amount of deionized water. The mixture of these two solutions was fed dropwise into a preheated (~80 $^o$C) aqueous solution of $Na_2CO_3$, which was prepared by dissolving 10 g of $Na_2CO_3$ in 300 mL of deionized water. The resulting solution was then cooled to room temperature and filtered; the cake retained on the filter was ground and calcined at 400 $^o$C for 12 hours.

Supported Pt catalysts were made by incipient wetness impregnation [18]. The $ZrO_2$ and ceria-promoted $ZrO_2$ supports were obtained from Magnesium Elektron Inc. (MEI) and were used as received. Pt was impregnated into the support at incipient wetness to give a Pt dosage between 0.5 to 1wt%. Catalysts were then dried at 110 $^o$C overnight and calcined in air (30 cm$^3$/min) for 2 hours at 400 $^o$C.

## 2.2 Catalytic reactivity testing

Prior to each run, the catalyst bed was pretreated under a thermal program in a stream containing 30 mole% of $H_2$ and 70 mole% of $N_2$. Cu/ZnO was reduced from room temperature to 250 $^o$C in a 4 $^o$C/min ramp and maintained at 250 $^o$C for an hour; supported Pt catalysts were reduced at 450 $^o$C in the same treatment stream for one hour.

A detail description about the experimental setup was reported in a previous publication [19] and only a brief summary is given here. Experiments were performed in a vertical quartz tube reactor inside a cylindrical furnace. Because of the high exothermicity of CPO, the catalyst bed was prepared by a mixture of 0.05 g sample with 0.45 g $SiO_2$ powder for every trial, sandwiched between plugs of quartz wool. $SiO_2$ powder is inert under reaction conditions used in this work. All catalysts and $SiO_2$ were pelletized, crushed and sieved into 40 to 45 mesh particles.

The composition of the gas stream at the entrance of reactor was 2.4 mole% $O_2$, 89.7 mole% of $N_2$ and 7.9 mole% methanol vapor, respectively. The $O_2/CH_3OH$ ratio was kept at 0.3. Five different gas hourly space velocities (GHSVs), 3800, 8000, 16 000, 24 000 and 40 000 hr$^{-1}$, were applied to test all catalysts. Catalytic results were acquired at 250 $^o$C. Gas hourly space velocity was calculated from [20]:

$$GHSV = \frac{\left(\text{Total gas flow rate at standard temperature and pressure}\right)}{\left(\text{volume of catalyst bed}\right)} \qquad (1)$$

For all data reported, the carbon and hydrogen mass balances closed within 10% error and most of them were under 5%. For each sample, three to five trials were taken. These multiple trials were used to estimate 95% confidence intervals. Selectivities of CO and $CO_2$ were based on carbon atoms; selectivities of $H_2$ and $H_2O$ were based on hydrogen atoms. Deactivation was not observed on supported Pt catalysts; however, it was observed for Cu/ZnO. Both activated and deactivated data for Cu/ZnO were recorded.

## 2.3 Kinetic modeling

A kinetic model was constructed for methanol CPO on Cu/ZnO and Pt/ZrO$_2$. This model assumed that the catalytic results could be modeled by the contribution of four reactions: methanol catalytic partial oxidation (CPO), methanol decomposition (MD), methanol steam reforming (MSR), and water-gas shift (WGS). CPO, MD, and MSR were found to form multiple products, so they were written as:

$$\text{CPO: } CH_3OH + \upsilon_{O_2,1}O_2 \rightarrow \upsilon_{CO,1}CO + \upsilon_{CO_2,1}CO_2 + \upsilon_{H_2,1}H_2 + \upsilon_{H_2O,1}H_2O \tag{2}$$

$$\text{MD: } CH_3OH \rightarrow \upsilon_{CO,2}CO + \upsilon_{CO_2,2}CO_2 + \upsilon_{H_2,2}H_2 + \upsilon_{H_2O,2}H_2O \tag{3}$$

$$\text{MSR: } CH_3OH + \upsilon_{H_2O,3}H_2O \rightarrow \upsilon_{CO,3}CO + \upsilon_{CO_2,3}CO_2 + \upsilon_{H_2,3}H_2 \tag{4}$$
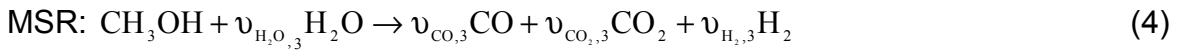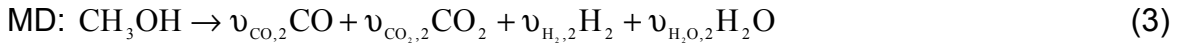
where $\upsilon_{O_2,i}$, $\upsilon_{CO,i}$, $\upsilon_{CO_2,i}$, and $\upsilon_{H_2O,i}$ are the stoichiometric coefficients of O$_2$, CO, CO$_2$, and H$_2$O, respectively (i = 1, 2, and 3).

The stoichiometric coefficients for CPO, MD, and MSR and the reaction rate constants for all four reactions were found from catalytic experiments. Prior to the catalytic investigations, influences from internal and external mass transfer resistances were investigated. Both of them are negligibly small except for external mass transfer resistance of Pt/ZrO$_2$: some difference (~ 10% in methanol conversion) was discovered at low space velocity, but leveled off at high GHSVs. The rate constants of MD, MSR, and WGS on Cu/ZnO and Pt/ZrO$_2$ were measured at GHSV = 16 000 hr$^{-1}$ over the catalyst bed with 0.05 g samples blended with 0.45 g SiO$_2$. CPO was estimated at GHSV = 40 000 hr$^{-1}$ over the catalyst bed with 0.01 g sample mixed with 0.49 g SiO$_2$. This was done to achieve incomplete oxygen composition in an attempt to limit secondary reactions that could complicate analysis. The O$_2$/CH$_3$OH ratio was kept at 0.3. The inlet molar composition was H$_2$O/CH$_3$OH = 1 for MSR and H$_2$O/CO = 1 for WGS.

The rate constant of each reaction was estimated using the integral method, MD was found to be first order, while all other reactions were second order. The stoichiometric coefficients were found by the ratio of the moles of a species reacted (for reactants) or produced (for products) divided by the moles of CH$_3$OH reacted. For example, the stoichiometric number of CO in CPO, MD, or MSR ($\upsilon_{CO,i}$) was found from:

$$\upsilon_{CO,i} = \frac{\text{mole of CO generated}}{\text{mole of CH}_3\text{OH consumed}} \tag{5}$$

The rate constants and experimental stoichiometric numbers of $O_2$, CO, $CO_2$, $H_2$ and $H_2O$ were incorporated into a packed bed reactor model. This model was solved using POLYMATH. Isothermal and isobaric conditions in the packed bed were assumed.

## 3. Results

3.1 Role of GHSV on Cu/ZnO and Pt/ZrO$_2$

Gas hourly space velocity can significantly affect product distributions [21,22]. Higher GHSV may mean that there is insufficient reaction time to reach equilibrium or for secondary reactions to occur, thereby changing which products are formed. Observing how product composition changes when GHSV is changed can, therefore, provide information on which reactions are primary reactions and which are secondary reactions.

It is known that Cu/ZnO catalysts deactivate during methanol partial oxidation [2,15,17]. Previous researchers suggested that sintering of Cu-Zn interface, oxidation of Cu, or deposition of carbonaceous species may cause the low stability of Cu/ZnO catalyst [15]. Because of the known stability problems of Cu/ZnO, deactivation was studied for three different space velocities.

Fig. 1 illustrates deactivation as a function of time-on-stream on Cu/ZnO with different space velocities. At GHSV = 3800 hr$^{-1}$, the selectivities of $CO_2$, $H_2$, and conversion of $CH_3OH$ decreased and formation of CO and $H_2O$ increased with reaction time. The same trends were found at GHSV = 8000 hr$^{-1}$; however, when 6% $O_2$ in $N_2$ was fed over the deactivated catalyst for 30 seconds, the original catalyst activity was regained. This is seen in Fig. 1 (b) at a time of ~300 minutes. At that time when a feed free of methanol is added, selectivities of $CO_2$, $H_2$, and conversion of $CH_3OH$ were greatly increased. Regeneration was only temporary, as the catalyst performance declined steadily once methanol was reintroduced.

While raising GHSV to 16 000 hr$^{-1}$, the selectivities of carbon oxides remained relative constant with time; on the contrary, $H_2$ selectivity declined dramatically, from ~78% to ~30% with reaction time. Again, regeneration was possible when methanol was removed from the feed: methanol conversion and $H_2$ selectivity both returned to their original values.
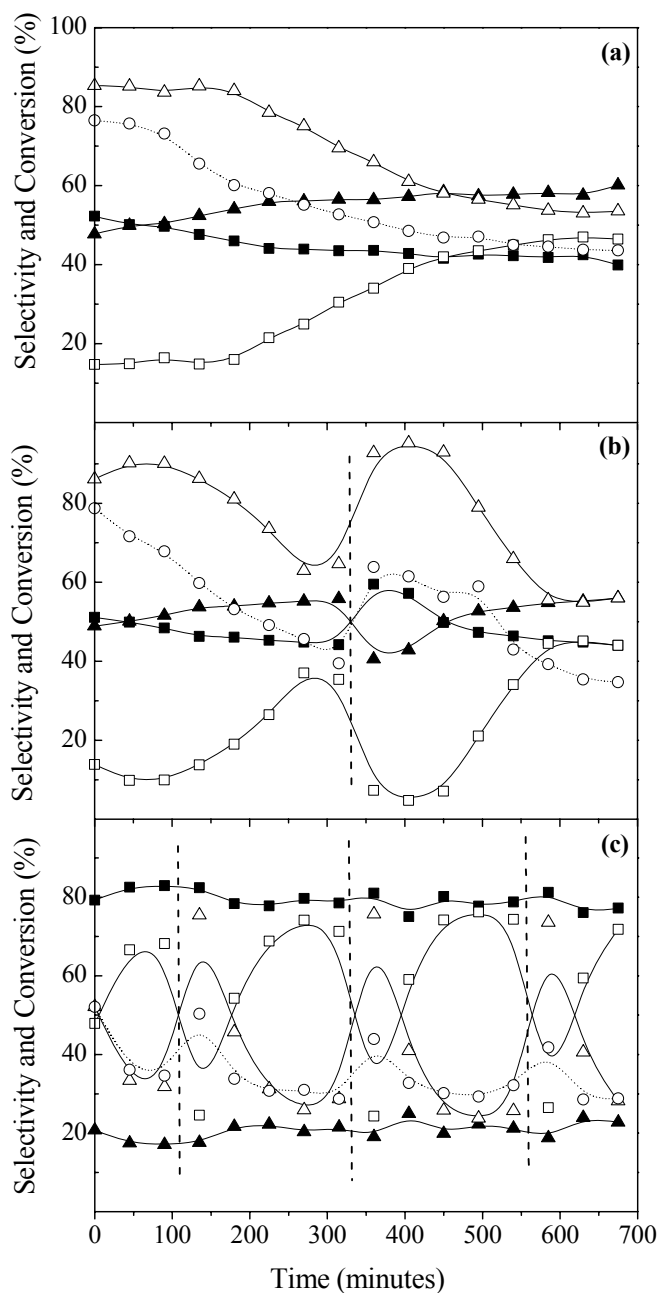
**Figure 1.** Selectivities of CO (▲), $CO_2$ (■), $H_2$ (△) and $H_2O$ (□) and conversion of $CH_3OH$ (o) as a function of time-on-stream in oxidation of methanol over Cu/ZnO at GHSV = (a) 3800, (b) 8000 and (c) 16 000 $hr^{-1}$. Dashed line indicated the time when $CH_3OH$ was removed from the feed.

Fig. 2 (a) presents the selectivities of CO and $CO_2$ on Cu/ZnO and Pt/ZrO$_2$ with different GHSV's. Cu/ZnO produced mainly $CO_2$ at all space velocities, while Pt/ZrO$_2$ produced mostly CO. With increasing GHSV, CO selectivity decreased

while $CO_2$ selectivity increased for both catalysts. CO selectivity on Cu/ZnO decreased from 39% at 3800 hr$^{-1}$ to 13% at 40 000 hr$^{-1}$, while CO selectivity on Pt/ZrO$_2$ decreased from 88% at 3800 hr$^{-1}$ to 80% at 40 000 hr$^{-1}$. Fig. 2 (b) shows the selectivities of $H_2$ and $H_2O$ on Cu/ZnO and Pt/ZrO$_2$. $H_2$ is the main product for both catalysts. As GHSV increased, $H_2$ selectivity on Cu/ZnO dropped sharply compared with that on Pt/ZrO$_2$. $H_2$ selectivity on Cu/ZnO decreased from 83% at 3800 hr$^{-1}$ to 62% at 40 000 hr$^{-1}$, while $H_2$ selectivity on Pt/ZrO$_2$ decreased from 70% at 3800 hr$^{-1}$ to 62% at 40 000 hr$^{-1}$.
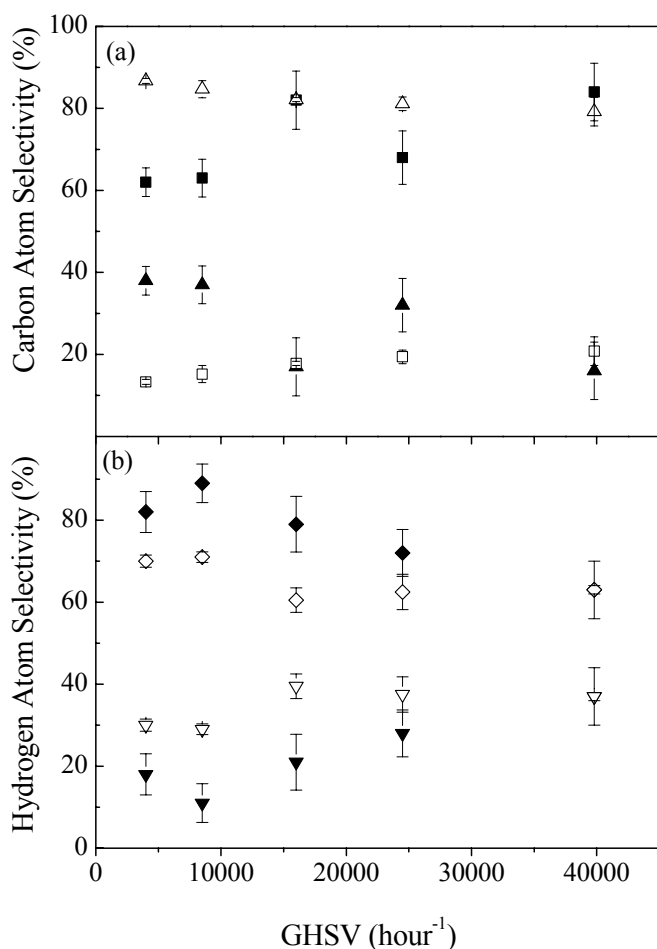


**Figure 2.** (a) Comparison of CO (▲) and $CO_2$ (■) selectivities on Cu/ZnO and CO (△) and $CO_2$ (□) selectivities on Pt/ZrO$_2$. (b) Comparison of $H_2$ (◆) and $H_2O$ (▼) selectivities on Cu/ZnO and $H_2$ (◇) and $H_2O$ (   ) selectivities on Pt/ZrO$_2$.

3.2. Kinetic modeling on Cu/ZnO and Pt/ZrO$_2$

To study why Cu and Pt catalysts give such different results and to better understand the influence of GHSV on product selectivity, the kinetics of four individual reactions that could be important in CPO were studied. Tables 1 and 2 summarize the rate constants and experimental stoichiometric numbers of CPO, MD, MSR and WGS over Cu/ZnO and Pt/ZrO$_2$ catalysts. CPO was about two times faster on Pt than Cu and MD proceeded approximately ten times faster on Pt than Cu, while MSD was roughly ten times faster on Cu than Pt. Rate constants of WGS were almost identical on both catalysts. Small amounts of byproducts, such as formaldehyde and methyl formate, were ignored in this kinetic determination.

**Table 1. Rate Constants of CPO, MD, MSR and WGS on Cu/ZnO and Pt/ZrO$_2$.**

| Catalyst | CPO ($L^2 \cdot mole^{-1} \cdot s^{-1} \cdot g_{cat}^{-1}$) | MD ($L \cdot s^{-1} \cdot g_{cat}^{-1}$) | MSR ($L^2 \cdot mole^{-1} \cdot s^{-1} \cdot g_{cat}^{-1}$) | WGS ($L^2 \cdot mole^{-1} \cdot s^{-1} \cdot g_{cat}^{-1}$) |
|---|---|---|---|---|
| Cu/ZnO | 14 700 | 0.0052 | 0.220 | 0.015 |
| Pt/ZrO$_2$ | 32 407 | 0.0510 | 0.036 | 0.020 |

**Table 2. Experimental Stoichiometric Number of each Product of CPO, MD, MSR and WGS over Cu/ZnO and Pt/ZrO$_2$.**

| | Cu/ZnO | | | | | Pt/ZrO$_2$ | | | | |
|---|---|---|---|---|---|---|---|---|---|---|
| | O$_2$ | H$_2$ | H$_2$O | CO | CO$_2$ | O$_2$ | H$_2$ | H$_2$O | CO | CO$_2$ |
| CPO | -0.8 | 1.2 | 0.8 | 0.2 | 0.8 | -0.6 | 1 | 1 | 0.8 | 0.2 |
| MD | 0 | 2 | 0 | 1 | 0 | 0 | 2 | 0 | 1 | 0 |
| MSR | 0 | 2.9 | -0.9 | 0.1 | 0.9 | 0 | 2.4 | -0.4 | 0.6 | 0.4 |
| WGS | 0 | 1 | -1 | -1 | 1 | 0 | 1 | -1 | -1 | 1 |

These reaction rate constants and experimental stoichiometric number were used in a packed bed reactor model to simulate CPO on Cu/ZnO and Pt/ZrO$_2$.

Fig. 3 shows the simulated reaction rates of CPO, MD, MSR and WGS as a function of position in the catalyst bed for Cu/ZnO and Pt/ZrO$_2$ at GHSV equal to 16 000 hr$^{-1}$. The trends for both catalysts were similar. CPO had the fastest reaction rate at the front end of catalyst bed, but reaction rate decreased dramatically as the oxygen was consumed. MD started to dominate the overall reaction after oxygen was depleted until the end of the catalyst bed. MSR and WGS reaction rates steadily increased until oxygen was fully consumed, then both rates reached a constant value through the rest catalyst bed. MSR and WGS had little impact on the overall reaction over the whole reaction zone due to their small reaction rates.
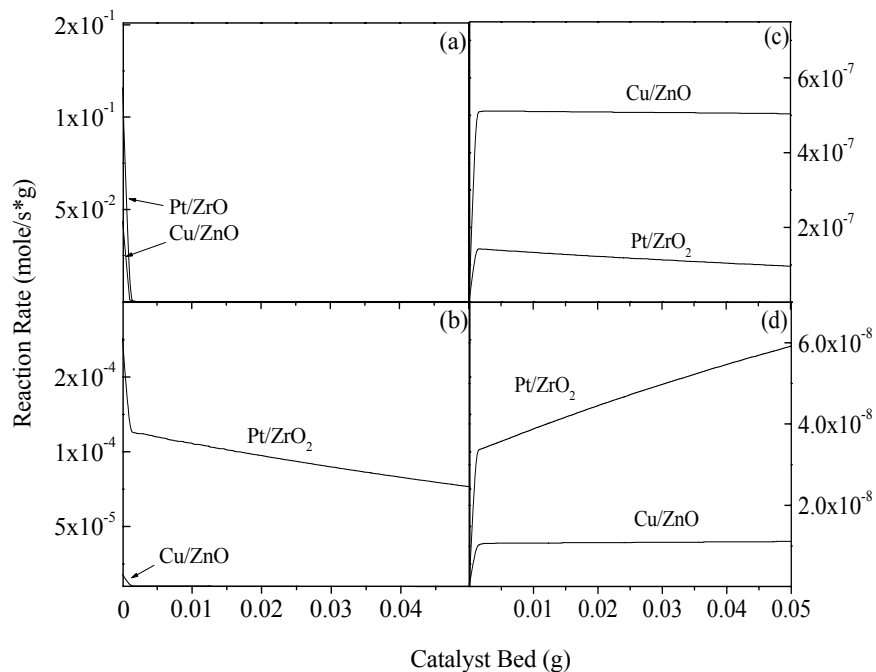
**Figure 3.** Simulated reaction rates of (a) CPO, (b) MD, (c) MSR and (d) WGS on Cu/ZnO and Pt/ZrO$_2$ at GHSV = 16 000 hr$^{-1}$.

Fig. 4 (a) shows the simulated molar flow rates of reactants and products as functions of position in the packed bed over a Cu/ZnO catalyst. Both reactants, CH$_3$OH and O$_2$, decreased rapidly while products, CO, CO$_2$, H$_2$ and H$_2$O increased at the entrance of catalyst bed. O$_2$ was depleted at about 0.003 g, where CPO ended and MD began to prevail. Once oxygen was completely spent, molar flow rates of reactants and products were relatively constant. For Pt/ZrO$_2$, shown in Fig. 4 (b), even though O$_2$ was reacted within 0.001 g of the catalyst bed, CO and H$_2$ molar flow rates continued to increase throughout the bed. This is not the case for CO$_2$ and H$_2$O.
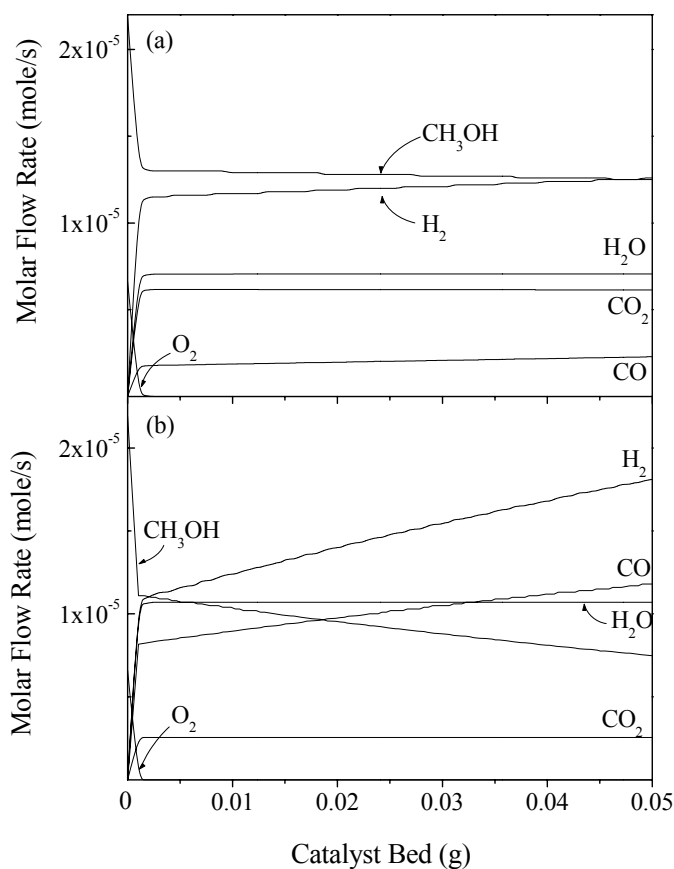
**Figure 4.** Simulated molar flow rates of reactants and products on (a) Cu/ZnO and (b) Pt/ZrO$_2$ at GHSV = 16 000 hr$^{-1}$.

The effect of GHSV on catalyst performance was simulated by varying the inlet flow rate used in the model. Fig. 5 displays both experimental and simulated methanol conversions over Cu/ZnO and Pt/ZrO$_2$ as function of GHSV. Oxygen conversion at every flow rate was close to 100%. For both simulations and experiments, conversions dropped with GHSV before leveling out at GHSV = 24 000 and 40 000 hr$^{-1}$.
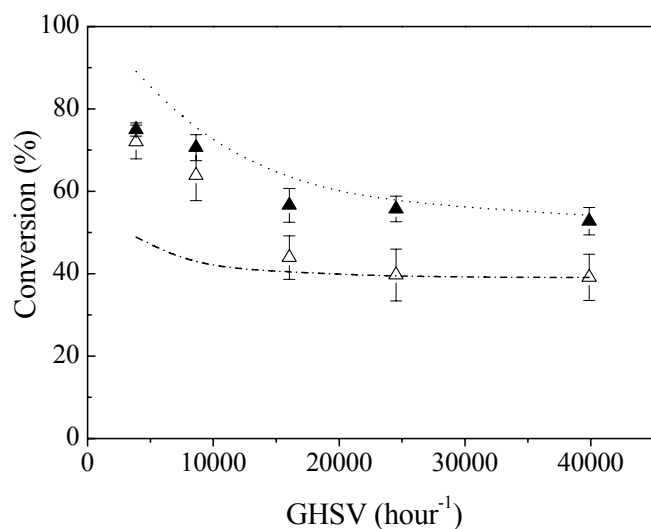
**Figure 5.** Methanol conversion of Cu/ZnO ($\triangle$), simulated Cu/ZnO (dash dot), Pt/ZrO$_2$ ($\blacktriangle$) and simulated Pt/ZrO$_2$ (dot).

Fig. 6 shows the simulated and experimental results for carbon atom selectivity on Cu and Pt catalysts. The simulated and experimental selectivites of CO and CO$_2$ are within 5% for all space velocities for Pt/ZrO$_2$ while the deviation between simulated and experimental data for Cu/ZnO is less than 15%. According to the 95% confidence, the models for Cu/ZnO and Pt/ZrO$_2$ agree with the experimental data since both of them are within the error bars and present the right trends. The trends of CO and CO$_2$ selectivities are similar to Pt/ZrO$_2$: increasing space velocity enhances CO$_2$ and decreases CO selectivities.
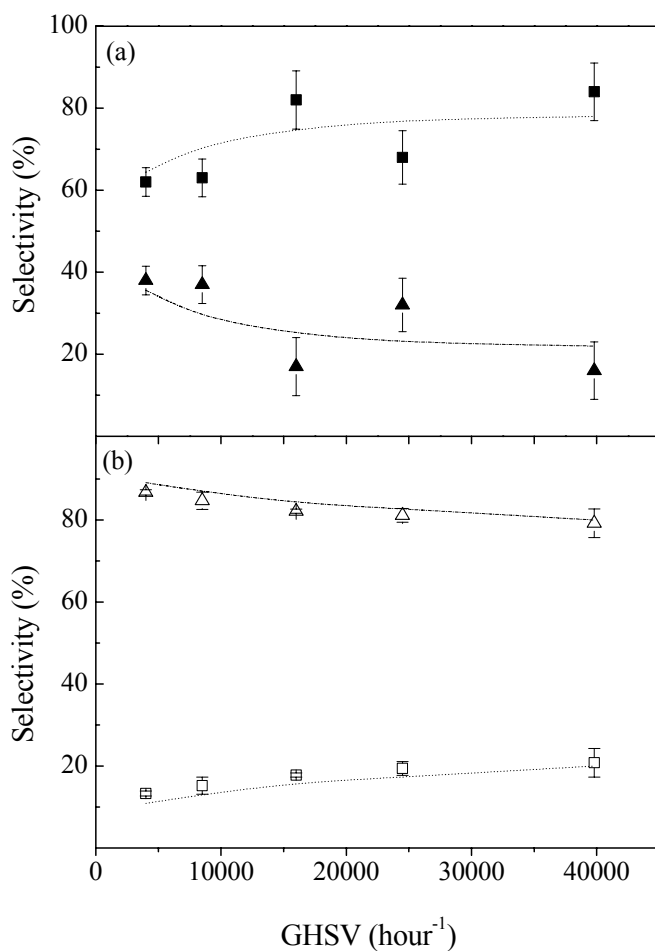
**Figure 6.** Comparison of simulated and experimental selectivities of (a) CO (dash dot and ▲) and $CO_2$ (dot and ■) on Cu/ZnO and (b) CO (dash dot and △) and $CO_2$ (dot and □) on Pt/ZrO$_2$.

Fig. 7 depicts the simulated and experimental selectivities of $H_2$ and $H_2O$ on Cu and Pt catalysts as GHSV is increased. Again, the experimental and simulated results are in excellent agreement for Pt/ZrO$_2$, but not for Cu/ZnO. For Cu/ZnO the model predicts little influence of GHSV, while experimentally $H_2$ selectivity drops dramatically as GHSV is increased. The model underestimates the selectivity of $H_2$ at low GHSVs.
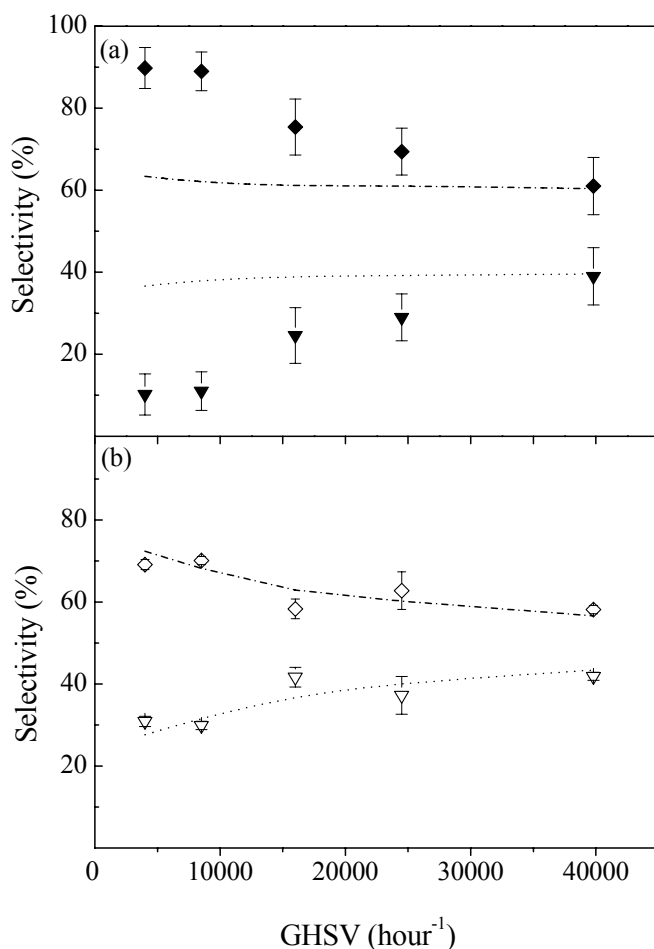
**Figure 7.** Comparison of simulated and experimental selectivities of (a) $H_2$ (dash dot and ◆) and $H_2O$ (dot and ▼) on Cu/ZnO and (b) $H_2$ (dash dot and ◇) and $H_2O$ (dot and   ) on Pt/ZrO$_2$.

## 4. Discussion

4.1 Differences between Cu/ZnO and Pt/ZrO$_2$

Catalytic partial oxidation of methanol on Cu/ZnO and Pt/ZrO$_2$ gave quite different products. The largest difference is that CPO over Cu/ZnO produced mostly $CO_2$, Pt/ZrO$_2$ produces CO. This is in agreement with literature results [12]. The simulation results provide an explanation for this difference.

In the simulation, CPO dominated reaction on both catalysts in the front of the packed bed. CPO was about two times faster on Pt/ZrO$_2$ than Cu/ZnO, despite the higher copper loading. After depleting oxygen, MD became the dominant reaction. The rate of MD was about one order of magnitude lower on Cu/ZnO than on Pt/ZrO$_2$. It generated only CO and $H_2$ on Pt/ZrO$_2$, leading to an

increase in their contents gradually through the catalyst bed. In contrast, the rate of MD was slower on Cu/ZnO. It formed not only CO and $H_2$, but also small amounts of $CO_2$, $H_2O$ and even formaldehyde and methyl formate [24]. Therefore, no significant change of CO and $H_2$ for Cu/ZnO was found in the rest of the catalyst bed. Both MSR and WGS were not fast enough to play a major role under the experimental conditions.

These results suggest that CPO and MD are the primary reaction pathways on both Cu/ZnO and $Pt/ZrO_2$. $Pt/ZrO_2$ produces a higher selectivity to CO than Cu/ZnO because the partial oxidation reaction produces more CO than Cu/ZnO and because methanol decomposition to CO and $H_2$ is a much faster reaction on $Pt/ZrO_2$.

4.2 Validity of kinetic model

While the kinetic model used in this work is empirical in nature, it fits the experimental data for $Pt/ZrO_2$ data quite well. It is unable to accurately represent Cu/ZnO, however. A major challenge for the model is representing what happens when methanol and oxygen react (CPO). Multiple reaction pathways occur during that process, but the model represents this complicated reaction as a single reaction with multiple products.  This approach worked well for $Pt/ZrO_2$, but not for Cu/ZnO. One possible explanation is that Cu/ZnO produced methyl formate and formaldehyde, while $Pt/ZrO_2$ did not. Since under typical experimental conditions (100% oxygen conversion) these products weren't detected, they were not considered in the model. In calculating the experimental stoichiometries for CPO, the formation of methyl formate and formaldehyde were ignored. These products obviously are converted to CO, $CO_2$, $H_2$, and $H_2O$, but we have not fully captured the way they do so.

4.3 Effect of GHSV on Cu/ZnO and $Pt/ZrO_2$

GHSV affected the catalytic results by changing the extents to which individual reactions contributed. The modeling results suggest that reaction occurs in two processes: the first when oxygen is present and the second after oxygen has been completely converted. CPO is important for all GHSV, since oxygen is always completely converted.  The other reactions have less influence at high GHSV. This explains why the CO and $H_2$ selectivities fall as GHSV is increased on both catalysts: there is less time for MD, which forms primarily CO and $H_2$, to occur. This effect is more significant on $Pt/ZrO_2$, since it is much more active for MD.

4.4 Deactivation on Cu/ZnO

Kung and his collaborators [15] have reported that sintering of CuO particles may be the cause of deactivation on the basis of surface area measurements and x-ray diffraction patterns. They also pointed out that carbonaceous deposits may play a role. Liu and his collaborators [8] have compared the deactivation

mechanisms of Cu/ZnO and Pd/ZnO. They found that selectivity to CO was constant during deactivation experiments on Cu/ZnO, while it increased during deactivation of Pd/ZnO. Hence, they suggested that the structural and chemical states of deactivated Cu/ZnO were the same as the active state.

According to our observations, Cu/ZnO can be reactivated by purging with $O_2$ in $N_2$, which may burn off the accumulated carbonaceous species on catalyst's surface. This might suggest that carbonaceous species are the main issue for deactivation.

## 5. Conclusion

Cu/ZnO and $Pt/ZrO_2$ catalysts gave different results in methanol CPO, with Cu/ZnO producing more $CO_2$ and $Pt/ZrO_2$ producing more CO. This difference is primarily due to the methanol decomposition reaction, which occurs roughly ten times faster on $Pt/ZrO_2$ than on Cu/ZnO, leading to additional production of CO and $H_2$ on $Pt/ZrO_2$. Methanol catalytic partial oxidation appears to proceed by two main pathways. The first occurs when oxygen is present, as methanol is converted to CO, $CO_2$, $H_2O$, and $H_2$. Once oxygen has been consumed, the second pathway, methanol decomposition, dominates. Water-gas shift and methanol steam reforming do not appear to play a significant role in catalytic partial oxidation of methanol at the conditions of this research.

## References

[1]  T-J. Huang, S-W. Wang, Appl. Catal. 24 (1986) 287.
[2]  S. Velu, K. Suzuki, T. Osaki, Catal. Lett. 62 (1999) 159.
[3]  S. Murcia-Mascarós, R.M. Navarro, L. Gómez-Sainero, U. Costantino, M. Nocchetti, J.L.G. Fierro, J. Catal. 198 (2001) 338.
[4]  S. Ellis, B.H. Sakakini, R. Torbati, K.C. Waugh, Catal. Lett. 82 (2002) 261.
[5]  M.C. Cubeiro, J.L.G. Fierro, J. Catal. 179 (1998) 150.
[6]  M.C. Cubeiro, J.L.G. Fierro, Appl. Catal. A 168 (1998) 307.
[7]  M. Borasio, O. Rodriguez de la Fuente, G. Rupprechter, H-J. Freund, J. Phys. Chem. B 109 (2005) 17791.
[8]  S. Liu, K. Takahashi, K. Fuchigami, K. Uematsu, Appl. Catal. A 299 (2006) 58.
[9]  R.W. McCabe, D.F. McCready, J. Phys. Chem. 90 (1986) 1428.
[10] M.P. Zum Mallen, L.D. Schmidt, J. Catal. 161 (1996) 230.
[11] A.W. Grant, J.H. Larsen, C.A. Perez, S.L. Lehto, M. Schmal, C.T. Campbell, J. Phys. Chem. B 105 (2001) 9273.
[12] B.E. Traxel, K.L. Hohn, Appl. Catal. A 244 (2003) 129.
[13] L.V. Mattos, F.B. Noronha, J. Catal. 233 (2005) 453.
[14] E.C. Wanat, B. Suman, L.D. Schmidt, J. Catal. 235 (2005) 18.
[15] E.D. Schrum, T.L. Reitz, H.H. Kung, Stud. Surf. Sci. Catal. 139 (2001) 229.
[16] T.L. Reitz, P.L. Lee, K.F. Czaplewski, J.C. Lang, K.E. Popp, H.H. Kung, J. Catal. 199 (2001) 193.
[17] L. Alejo, R. Lago, M.A. Pena, J.L.G. Fierro, Appl. Catal. A 162 (1997) 281.

[18] S.M. Stagg-Williams, R. Soares, E. Romero, W.E. Alvarez, D.E. Resasco, Stud. Surf. Sci. Catal. 130 (2000) 3663.

[19] Y-C. Lin, K.L. Hohn, Catal. Lett. 107 (2006) 215.

[20] H.S. Fogler, Elements of Chemical Reaction Engineering, 3rd ed., Prentice-Hall International, NJ, 1999.

[21] P.D.F. Vernon, M.L.H. Green, A.K. Cheetham, A.T. Ashcroft, Catal. Today 13 (1992) 417.

[22] S.S. Bharadwaj, L.D. Schmidt, Fuel Process. Technol. 42 (1995) 109.

[23] S. Velu, K. Suzuki, Top. Catal. 22 (2003) 235.

[24] A.Y. Rozovskii, G.I. Lin, Top. Catal. 22 (2003) 137.